

Article

Exploration of Pyrolysis Behaviors of Waste Plastics (Polypropylene Plastic/Polyethylene Plastic/Polystyrene Plastic): Macro-Thermal Kinetics and Micro-Pyrolysis Mechanism

Weiwei Xuan *, Shiyong Yan and Yanwu Dong

School of Energy and Environmental Engineering, University of Science and Technology Beijing, Beijing 100083, China; m202120252@xs.ustb.edu.cn (S.Y.); g20208210@xs.ustb.edu.cn (Y.D.)

* Correspondence: xww@ustb.edu.cn; Tel.: +86-010-62332730

Abstract: Pyrolysis is a promising technology used to recycle both the energy and chemicals in plastics. Three types of plastics, polyethylene plastic (PE), polypropylene plastic (PP) and polystyrene plastic (PS) were investigated using thermogravimetry–mass spectrometry (TG–MS) and reactive force field molecular dynamics (ReaxFF-MD) simulation. The thermogravimetric analysis showed that all three plastics lost weight during the pyrolysis in one step. The thermal decomposition stability is PS < PP < PE. The activation energies and reaction mechanism function of the three plastics were determined by the Kissinger and CR methods. Meanwhile, the ReaxFF-MD combined with density functional theory (DFT) was used to calculate the kinetics, as well as explore the pyrolysis mechanism. The calculated kinetic results agree well with the experimental methods. The common pyrolysis reaction process follows the dissociation sequence of the polymer to polymeric monomer and, then, to the gas molecules. Based on the bond length between the monomers and the bond dissociation energy for different plastics, the required energy for polymer dissociation is PS < PP < PE, which microscopically explains the macro-activation energy sequence and thermal stability. Moreover, due to the retention of aromatic rings in its monomers, PS almost completely converts into oil.

Keywords: waste plastics; pyrolysis kinetics; TG–MS; ReaxFF-MD; DFT



Citation: Xuan, W.; Yan, S.; Dong, Y. Exploration of Pyrolysis Behaviors of Waste Plastics (Polypropylene Plastic/Polyethylene Plastic/Polystyrene Plastic): Macro-Thermal Kinetics and Micro-Pyrolysis Mechanism. *Processes* **2023**, *11*, 2764. <https://doi.org/10.3390/pr11092764>

Academic Editor: George Z. Kyzas

Received: 29 August 2023

Revised: 12 September 2023

Accepted: 13 September 2023

Published: 15 September 2023



Copyright: © 2023 by the authors. Licensee MDPI, Basel, Switzerland. This article is an open access article distributed under the terms and conditions of the Creative Commons Attribution (CC BY) license (<https://creativecommons.org/licenses/by/4.0/>).

1. Introduction

Plastics are a kind of synthetic polymer compound mainly made from raw petrochemical products, which have been widely used in production and living. In 2018, global plastic production reached 359 million tons, with China alone accounting for nearly 30% [1,2]. Actually, plastics, especially PE, PP and PS with high calorific value, are widely used in packaging and the building materials industry [3]. With the increasing use of plastics, waste disposal has become a thorny issue. At present, the simplest treatment methods include direct incineration and land filling, but these methods cause serious air pollution and soil pollution [4]. Thermochemical transformation technologies, such as pyrolysis, are promising treatment methods to recycle high energy carriers. Waste plastic is heated to a medium temperature in an inert atmosphere and thermally cracked, producing high value-added chemical products, such as oil [5–7]. Generally speaking, pyrolysis is affected by temperature, pressure, the heating rate, reaction time, the catalyst and other factors, so it is necessary to clarify the detailed mechanism and reaction kinetics.

Thermogravimetric (TG) analysis is a common method used to study the pyrolysis kinetics of solid materials. The combination of TG data and mathematical model fitting can be used to calculate the kinetic parameters of the pyrolysis reaction, and help to deduce and verify the reaction mechanism [8–11]. Pan et al. used the TG–FTIR–MS experimental method to study the pyrolysis characteristics of PVC plastic at a temperature of 200–900 °C and analyzed the kinetics of PVC using the KAS, FWO and FR methods [12]. He et al. found that when PP or PE is pyrolyzed alone, its monomer structure is first generated,

followed by corresponding alkanes and small molecule gases [13]. Hu et al. studied the co-pyrolysis characteristics of HDPE, LDPE, PP and PS, and waste tires using TG–FTIR, and explored the thermal decomposition behavior, dynamic transformation and gas release characteristics of the pyrolysis process. The co-pyrolysis process can be divided into three stages, according to the reaction activation energy, by using the first-order reaction kinetics model [14]. Singh S et al. conducted thermogravimetric analysis (TGA) experiments on a single and mixed pyrolysis of corn cob (CC) and polyethylene plastic (PE) to investigate the thermal response, kinetics, reaction mechanism and thermodynamics of the pyrolysis process. The activation energy in the process was calculated using different models, such as Kissinger, Friedman, Starink, Vyazovkin and others, and it was found that the variation in the reported values on the activation energy was not significantly different [15]. However, the experiment can hardly capture the detailed conversion of radicals at the atomic level and reveal the difference in the pyrolysis mechanism of various plastics.

With the progress in computer technology and the development of a reactive force field, which can describe chemical reactions [16], molecular dynamics simulation plays an important role in the study of the reaction mechanism because of its good microscopic visualization effect and the applicability of large-scale atoms [17]. This method uses the distance between atoms to obtain the bond level and bond energy, and describes chemical reactions from the perspective of bond generation and fracture without the definition of the reaction path in advance. It has been widely used in the mechanism studies on coal, biomass, polymers and other complex macromolecules [18–23]. Batuer et al. proposed a new ReaxFF molecular dynamics simulation model to predict the volatility and coke evolution during cotton pyrolysis using isothermal simulation and the volatile variable removal rate (VRR) [24]. Liu et al. constructed a pyrolysis system containing eight PE chains, and verified the accuracy of the ReaxFF-MD simulation by comparing the simulated product distribution with the experimental Py–GC/MS results. The detailed reaction mechanism and gas molecule generation pathway of PE pyrolysis were obtained through simulation track analysis at the micro-atomic level [25]. Xu et al. used MD to investigate the pyrolysis pathways of PE under non-isothermal and isothermal conditions [26]. Also, Wang et al. studied the co-pyrolysis mechanism of biomass and PE using MD and density functional theory (DFT) and the synergistic effect of the co-pyrolysis of coal and PE/PS was studied using MD [27,28]. Xuan et al. discovered the steam gasification mechanism of PE using MD and revealed the bond energy at different positions [29]. Therefore, the ReaxFF-MD method coupled with DFT can effectively reveal the chemical reaction mechanism of thermal conversion at the micro level.

Different plastics have different thermal behaviors; the products also vary depending on the chemical structures of the plastic types [30,31]. However, pyrolysis mechanisms have rarely been compared and explained at the molecular level. Understanding the structural evolution of different plastic types during thermal treatment is helpful to improve the reaction process and achieve more high-value oil and gas during co-pyrolysis/gasification. In this paper, thermogravimetry–mass spectrometry (TG–MS) was first used for the experimental analysis of three representative plastics, namely PE, PP and PS. Then, the Kissinger and Malek plus CR kinetic methods were used to determine the pyrolysis kinetic parameters. Meanwhile, the ReaxFF-MD simulation combined with DFT was performed to explore the reaction kinetics verified by the TG experiment. The radical evolutions and pyrolysis mechanisms of the three plastics were revealed on the micro-atomic level. The energy barriers of key reactions for producing pyrolysis oil and gaseous products were calculated using transition state calculations based on DFT. Through comparing the energy barriers, the macro-kinetics of the three plastics determined from the TG experiment are explained. These studies can provide theoretical support and basic kinetic data for the optimization of the plastic pyrolysis process and reactor design.

2. Methods

2.1. Experiment

2.1.1. Experimental Materials and Methods

Three plastic powders, PE, PP and PS, with a particle size of 100 mesh were dried in a vacuum drying oven at 105 °C for 2 h. The ultimate analysis and the proximate analysis of the samples are shown in Table 1. Then, the dried waste plastics were analyzed by a synchronous thermal analyzer (STA 449F3) coupled with an online quadrupole mass spectrometer (QMS 403 D). For the TG–MS experiment, 10 mg of the plastic sample was placed in an alumina crucible to heat up from room temperature to 150 °C, with a heating rate of 10 °C/min, and held for 40 min. Then, the heating rate continued to rise to 800 °C at 5, 10 and 15 °C/min, respectively. Argon gas was used as the carrier gas with an 80 mL/min flow rate to provide an inert atmosphere for pyrolysis. Each experiment was repeated three times to eliminate the interference from the equipment and human factors.

Table 1. Proximate and ultimate analysis of waste plastics.

Plastic	Proximate Analysis	Proportion (wt%)	Ultimate Analysis	Proportion (wt%)
PE	C	85.12	Fixed carbon	0
	H	14.12	Moisture	0.12
	N	0	Volatile	99.88
	S	0.14	Ash	0
PP	C	85.26	Fixed carbon	0.05
	H	14.19	Moisture	0.12
	N	0	Volatile	99.83
	S	0.43	Ash	0
PS	C	91.41	Fixed carbon	0
	H	7.82	Moisture	0.12
	N	0	Volatile	99.88
	S	0.20	Ash	0

2.1.2. Kinetic Calculation Theory

The non-isothermal solid pyrolysis process can be described with the Arrhenius Equation [32]:

$$\frac{d\alpha}{dt} = \beta \cdot \frac{d\alpha}{dT} = A \cdot \exp^{-\frac{E_a}{RT}} \cdot f(\alpha) \quad (1)$$

where α is the solid reaction conversion rate; t is the reaction time, min; E_a is the activation energy, kJ/mol; A the pre-exponential factor min^{-1} ; $f(\alpha)$ is the reaction mechanism function; β is the constant heating rate, K/min; T is the reaction temperature, K; and R is the universal gas constant, 8.314 J/(mol·K).

Kissinger Method

The greatest advantage of the Kissinger method is the preliminary estimation of the activation energy and pre-exponential factors when the pyrolysis mechanism function is unknown [32]. According to the data, at the maximum conversion rate for multiple TG curves measured at different heating rates, linear fitting analysis was performed on the characteristic values of the pyrolysis thermogravimetric experiment. After the integration of Equation (1), the standard Kissinger equation can be derived as follows:

$$\ln\left(\frac{\beta}{T_{\max}^2}\right) = -\frac{E}{RT_{\max}} + \ln\left(\frac{AR}{E}\right) \quad (2)$$

where T_{\max} is the peak (maximum) temperature obtained in the DTG curves, K.

Combination of the Malek and Coats–Redfern Methods

The Malek and Coats–Redfern (CR) methods are commonly combined to study the thermal decomposition process of polymers. The combination of two methods can reduce the trouble of trying reaction mechanism functions one by one [33].

In this paper, the Malek method was used to compare the fitting curve of the pyrolysis experimental data points with the standard curves of 20 common mechanism functions (shown in Supplementary Table S1) [10,11,34]. Then, the standard curve that matched the fitting curve the most was determined as the reasonable mechanism function for pyrolysis. The thermogravimetric experiment data can be converted into the defined function $y(\alpha)$ by Equation (3a) and the theoretic function can be determined by Equation (3b):

$$y(\alpha) = \left(\frac{T}{T_{0.5}}\right)^2 \cdot \frac{\frac{d\alpha}{dt}}{\left(\frac{d\alpha}{dt}\right)_{0.5}} \quad (3a)$$

$$y(\alpha) = \frac{f(\alpha)g(\alpha)}{f(\alpha)_{0.5}g(\alpha)_{0.5}} \quad (3b)$$

where $T_{0.5}$, $\left(\frac{d\alpha}{dt}\right)_{0.5}$, $f(\alpha)_{0.5}$ and $g(\alpha)_{0.5}$ are, respectively, the temperature, weight loss rate, differential and integral forms of the mechanism functions when the conversion rate is $\alpha = 0.5$.

According to the mechanism function model determined by the Malek method, the Coats–Redfern (CR) method was used to perform linear fitting analysis on the data obtained from the TG experiment [35]. After integration, the standard CR equation can be deduced as:

$$\ln\left(\frac{g(\alpha)}{T^2}\right) = -\frac{E}{RT} + \ln\left[\frac{AR}{\beta E}\left(1 - \frac{2TR}{E}\right)\right] \approx -\frac{E}{RT} + \ln\left(\frac{AR}{\beta E}\right) \quad (4)$$

where $g(\alpha)$ is the integral form of the reaction mechanism function. Through linear fitting, the activation energy E and the pre-exponential factor A can be determined by the slope and intercept.

2.2. Simulation Details for ReaxFF-MD and DFT

2.2.1. Model Construction

In reality, plastic is composed of thousands of atoms. But, due to limitations to computing power, we need to build a suitable model through practical simulations. Knyazev V.D. and Smith K.D. et al. studied the effect of the molecular weight of the PE chain on the initial C–C bond dissociation rate and found that the dissociation rate increased dramatically when the number of ethylene monomers was less than 5, but gradually became saturated when the degree of polymerization was further increased [36,37]. Our previous study on the steam gasification of PE plastic proved that the model, $C_{50}H_{102}$, can be a good representative in comparison to ReaxFF-MD with experiments [29]; therefore, a long chain model composed of at least fifty C atoms was constructed using Materials Studio software for PE, PP and PS plastics. The content of S is low in Table 1 and, thus, it is ignored in the model. The molecular formulas of the three plastics are $C_{50}H_{102}$, $C_{51}H_{104}$ and $C_{56}H_{58}$, respectively.

After geometric optimization using the Forcite module, the 20 optimized polymer chains were put together in a cubic periodic cell, employing the construction function in the Amorphous Cell program. In addition, the periodic boundary conditions were used to eliminate possible boundary effects. The PE, PP and PS pyrolysis systems are constructed in Figure 1, respectively.

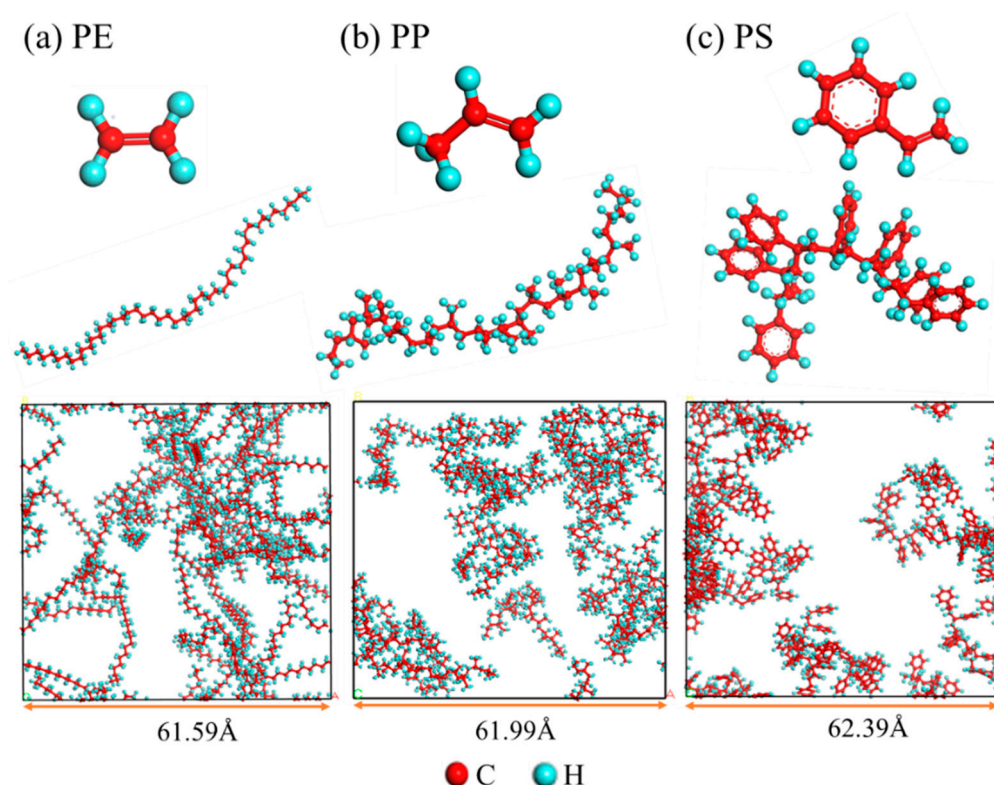


Figure 1. Monomers and pyrolysis reaction systems for (a) PE, (b) PP and (c) PS.

2.2.2. Simulation Details

In this paper, the ReaxFF-MD method was used to simulate the pyrolysis of plastics, based on the LAMMPS software. Firstly, the system was equilibrated at a low temperature, 300 K for 100 ps, to obtain a reasonable initial reaction system. In the non-isothermal pyrolysis simulation, the reaction system was gradually heated from 300 K to 3000 K at a constant heating rate of 10 K/ps. For the isothermal pyrolysis simulation process, the temperature of the simulation system was rapidly increased to high temperature ranges of 2500–3500 K. When the system reached a high temperature, the NVT ensemble was applied and the N-H method was used to control the system at a specified temperature [38]. The simulations were performed at different temperatures to obtain the reaction rates and activation energy. In an MD simulation, the temperature is usually increased to accelerate the reaction rate, which has been widely used in the study of oxidation and pyrolysis of hydrocarbons and biomass [22,39,40]. The calculated weight curve is verified with the TG results. During the ReaxFF-MD simulation process, the C/H/O reaction field [40] was used to describe the chemical reaction. The visualization software OVITO was used to observe and analyze the reaction process.

In order to further discuss the product conversion and reaction paths obtained by the ReaxFF-MD, the DMol3 module and DFT theory in the Materials Studio software are used to calculate the dissociation energy of some important bonds in the reaction process. The BLYP (Becke–Lee–Yan–Parr) functional at the generalized gradient approximation (GGA) level is used in the calculation [41]. The base group is set to DNP, and the convergence criteria of the energy, maximum force and maximum displacement are set to 1×10^{-5} Hartree, 2×10^{-3} Hartree/Å and 5×10^{-3} Å, respectively [42]. We also use the DFT calculation method to calculate the reaction energy barrier of each path in the process of product formation. Here, the reaction energy barrier is defined as [43]:

$$E_{\text{barrier}} = E_{\text{ts}} - E_r$$

where E_{barrier} is the energy barrier of the reaction, kJ/mol; E_{ts} is the energy kJ/mol of the transition state product; and E_r is the energy of the reactant, kJ/mol.

3. Results and Discussion

3.1. Study on Pyrolysis by Experiment

3.1.1. TG–MS Analysis

Figure 2a shows the TG and DTG curves for the three plastics. It can be seen that the pyrolysis process has only one weight loss peak, and the weight loss basically reaches 100%. At higher heating rates, the TG and DTG curves for the three plastics move to the right, and the solid weight loss is faster. The right shift in the pyrolysis curve can be explained by thermal hysteresis when the heating rate is high. The decomposition temperature of PE, PP and PS ranges from 456–496 °C, 412–478 °C and 389–431 °C, respectively. The gas release from the plastics during pyrolysis at 10°C/min was monitored online by MS and the results are shown Figure 2b. Since most products from PS are found in oil, only the gases from PE and PP are monitored [44,45]. The temperature range is basically consistent with the pyrolysis weight loss, and the peak temperatures for PE and PP are 481 °C and 463 °C, respectively. The main types of monitored gas being released are C_3H_6 ($m/z = 42$), C_2H_4 ($m/z = 28$), H_2 ($m/z = 2$) and CH_4 ($m/z = 16$) gases, which were also detected by Qin et al. in their experimental study of plastic pyrolysis [46].

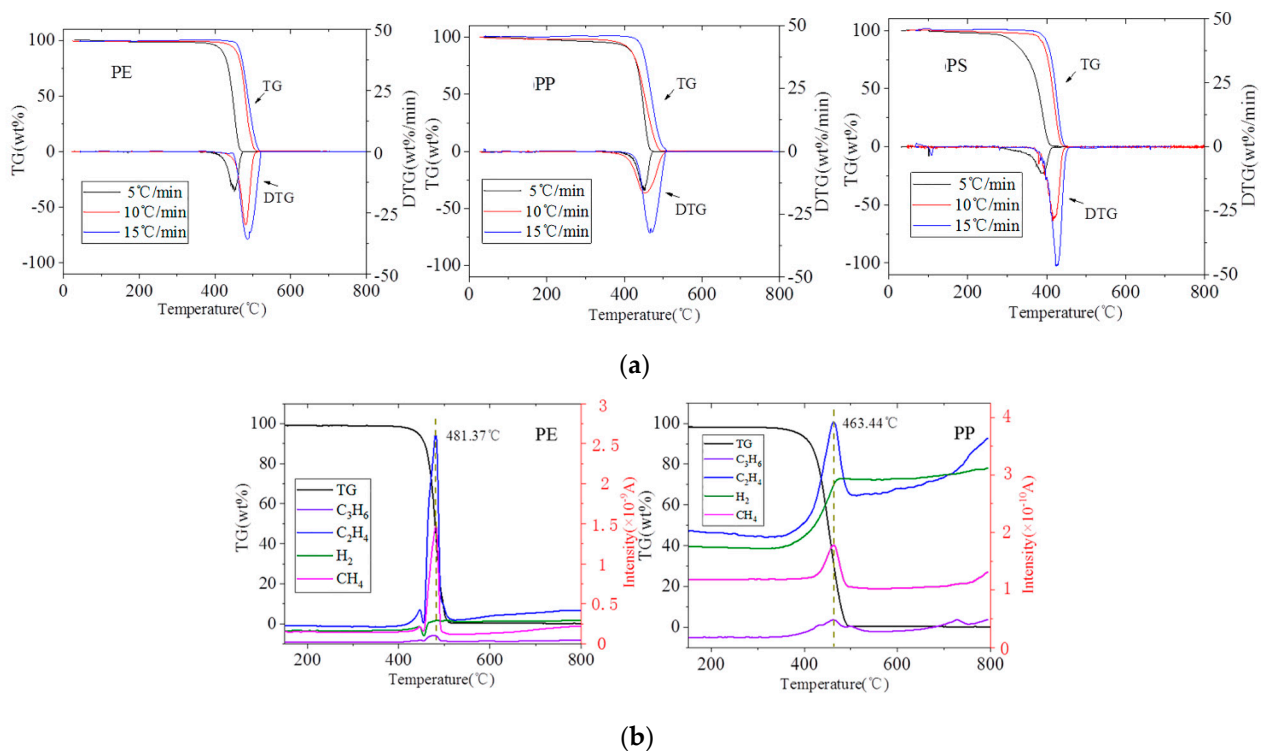


Figure 2. TG–MS results: (a) TG curves and (b) MS curves.

3.1.2. Kinetic Analysis

Kissinger Method

The Kissinger method is used to fit and predict the activation energy of the pyrolysis reaction. According to Equation (2), linear fitting of $\ln\left(\frac{\beta}{T_{\text{max}}^2}\right)$ to $\frac{1000}{T_{\text{max}}}$ at different heating rates was performed and the results are shown in Table 2. From the activation energy results, PS is relatively easier to perform pyrolysis, while PE requires the highest energy to react.

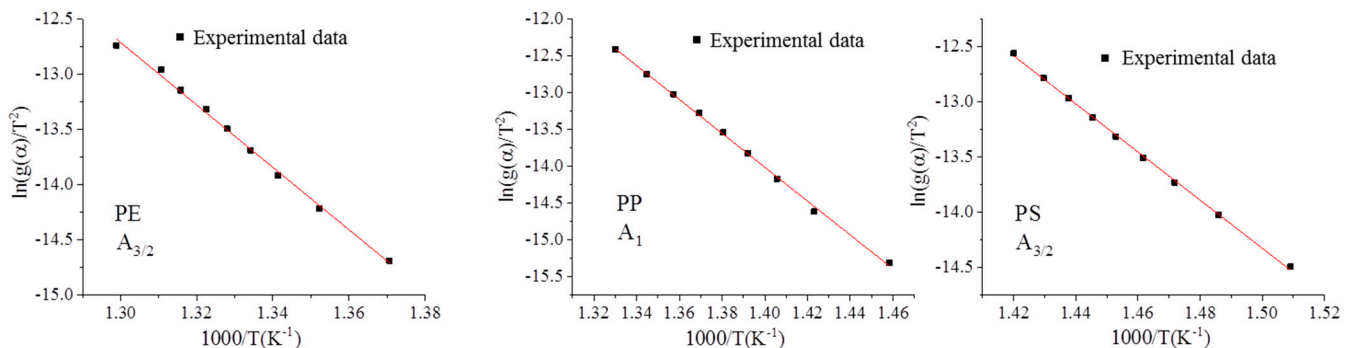
Table 2. Characteristic parameters of plastic pyrolysis and the kinetic parameters predicted by the Kissinger method.

Plastic	B (K/min)	T_{max} (K)	α_{max}	E (kJ/mol)	A (min^{-1})	R^2
PE	5	465.83	0.64	228.74	3.63×10^{12}	0.948
	10	481.37	0.56			
	15	486.09	0.49			
PP	5	446.80	0.54	193.43	2.30×10^{10}	0.994
	10	463.46	0.55			
	15	471.2	0.55			
PS	5	401.68	0.63	181.63	2.73×10^{10}	0.997
	10	416.22	0.53			
	15	423.77	0.52			

Combination of the Malek and CR Method to Determine the Kinetics

The Malek method is used to determine the reaction mechanism model. The differential $f(\alpha)$ and integral $g(\alpha)$ forms corresponding to 20 kinetic mechanism functions are used in Equation (3). And then, the theoretical and experimental fitting curves are compared (shown in Supplementary Figure S1). The best fitting correlations (No. 4–11) are found.

Since the determined reaction mechanism model corresponds to multiple equations, it is necessary to further determine the exact reaction mechanism equation. Different integral forms $g(\alpha)$ of the No. 4–11 mechanism equations were used in Equation (4) and the linear fitting of the experimental $\ln(\frac{g(\alpha)}{T^2})$ against $\frac{1000}{T}$ was carried out. The best fitting curve was selected to determine the kinetics. Figure 3 shows the comparison of the most suitable mechanism function with the experimental data. The calculated kinetics data and reaction mechanism are summarized in Table 3.

**Figure 3.** Linear fitting of the mechanism function of the PE, PP and PS plastics using the CR method.**Table 3.** Kinetic parameters of the plastic pyrolysis reaction.

	Methods	PE	PP	PS
E (kJ/mol)	Kissinger	228.74	193.43	181.63
	CR	234.90	191.45	181.21
	ReaxFF-MD	224.31	195.03	176.26
$\ln A$ (min^{-1})	Kissinger	3.63×10^{12}	2.30×10^{10}	2.73×10^{10}
	CR	7.60×10^{12}	1.90×10^{10}	2.06×10^{10}
Mechanism function		$A_{3/2}$	A_1	$A_{3/2}$

3.2. Study on the Pyrolysis by ReaxFF-MD

3.2.1. Model Verification

Firstly, the pyrolysis weight loss curve for the three plastics was calculated using ReaxFF-MD simulation and the results were compared with the TG experimental results. In molecular dynamics simulation, the state of organic species is commonly defined as: C_{40+} as solid, C_5 – C_{39} as liquid and C_1 – C_4 as gas [47].

As shown in Figure 4, the simulated weight loss process is basically consistent with the TG experimental results. In the ReaxFF-MD simulation, the initial weight loss temperature sequence of the different plastics is PS (2002 K) < PP (2069 K) < PE (2149 K), which agrees with the TG results, as PS (389 °C) < PP (412 °C) < PE (456 °C). The reason for the higher simulated temperature is mainly caused by the small-time scale of the ReaxFF-MD method. The agreement of the weight loss curve with the TG results shows that the three constructed reaction models are suitable for pyrolysis simulation.

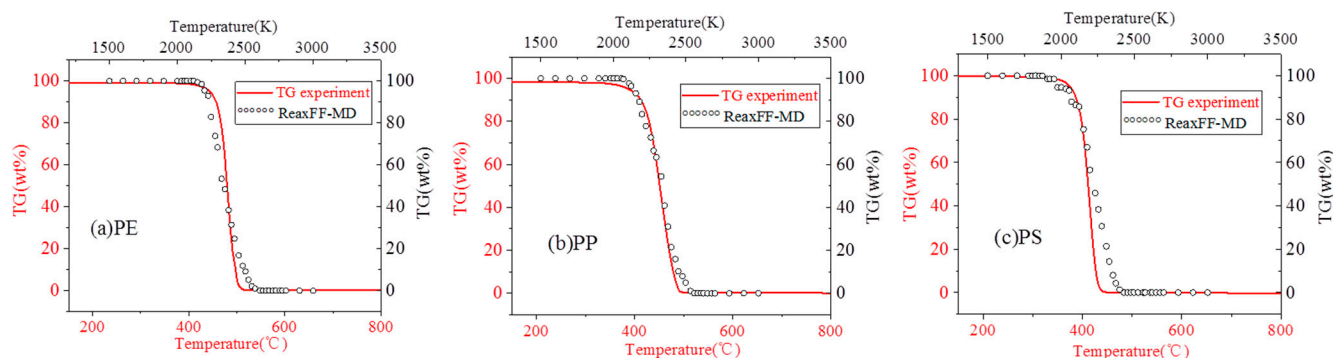


Figure 4. A comparison between the weight loss curve for the three plastics using ReaxFF-MD and TG experiment.

3.2.2. Kinetic Analysis

Then, the pyrolysis kinetics of the PE, PP and PS plastics are calculated using ReaxFF-MD simulation. Taking the PE plastic as an example, the pyrolysis reaction process of the polymer can be expressed as follows:



where $C_{50}H_{102}$ represents the PE plastic. In the simulation, the reaction concentration can be represented by the number of PE chains, and the reaction time can be calculated from the occurrence of the first PE chain dissociation to the time when 90% of the PE chain dissociation occurs [11,48]. The reaction rate for this process can be expressed by the following formula:

$$\ln(N_0) - \ln(N_1) = k(T) \cdot (t_0 - t_1) \quad (6)$$

where N_0 represents the number of PE chains at the beginning, N_1 represents the number of remaining PE chains when the PE dissociation conversion rate reaches 90%, T_0 represents the moment when the first PE chain begins to dissociate, and T_1 represents the moment when the PE dissociation conversion rate reaches 90%.

Furthermore, according to the Arrhenius equation and Equation (6), the pre-exponential factor A and activation energy E can be determined by the slope and intercept of the fitting line $\ln(k(T))$ against $\frac{1000}{T}$. Similarly, the kinetics of PP and PS are calculated. The fitting lines are shown in Figure 5.

Table 3 lists the kinetic results from the ReaxFF-MD simulation, as well as the Kissinger and CR methods. From Figure 6, we can see that the kinetic results from different methods are similar and the errors are within 5%. For the three different plastics, the sequence $E_{PS} < E_{PP} < E_{PE}$ indicates that PE has the highest thermal stability, while the PS plastic is the most reactive. This is in accordance with the TG-MS experiment, where the decomposition temperature range for PS is the lowest, while that of PE is the highest.

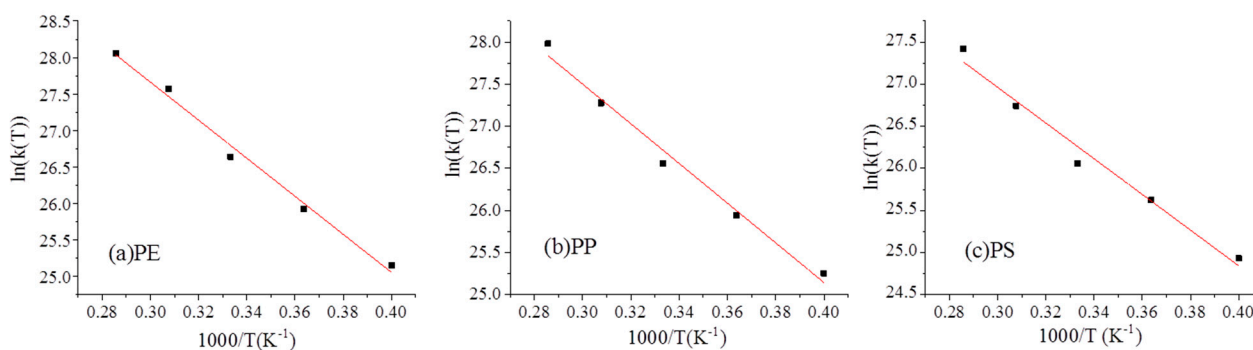


Figure 5. Kinetic analysis of PE, PP and PS plastics using ReaxFF-MD.

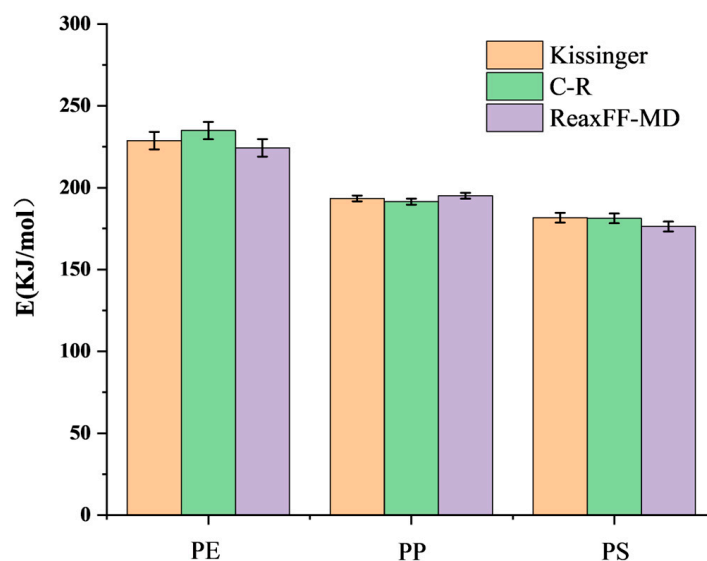


Figure 6. Error results.

3.2.3. Product Distribution

The statistics on the product distributions with the temperature of the three plastics are shown in Figure 7a–c. For the PE and PP plastics, oil and gas almost occur at the same time and the highest oil yield can reach nearly 50 wt%. But when the temperature exceeds 2500 K, the oil starts to crack continuously and, finally, almost completely converts into gas. However, for PS, most of the solids transform into oil, while little gas is generated. By tracing the transformation of styrene monomers, we found that only 2.14% of the aromatic rings are converted into small hydrocarbons by the ring-opening reaction at the end of weight loss, therefore most are completely converted into oil. This is consistent with previous experimental results, where nearly 95% oil can be obtained in different pyrolysis operational conditions for PS plastic [11,49]. The composition of the gases derived from the pyrolysis of the three plastics is shown in Figure 7d, the results of which are consistent with the MS results. PE and PP are very similar in terms of the gases formed, mainly their respective monomers ethylene and propylene, which account for nearly 80% of the total. The pyrolytic gases from the PS plastic are much less and lag more than other plastics, are mainly composed of acetylene and hydrogen, and are mainly produced by the dehydrogenation reaction of vinyl after breaking the C–C bond.

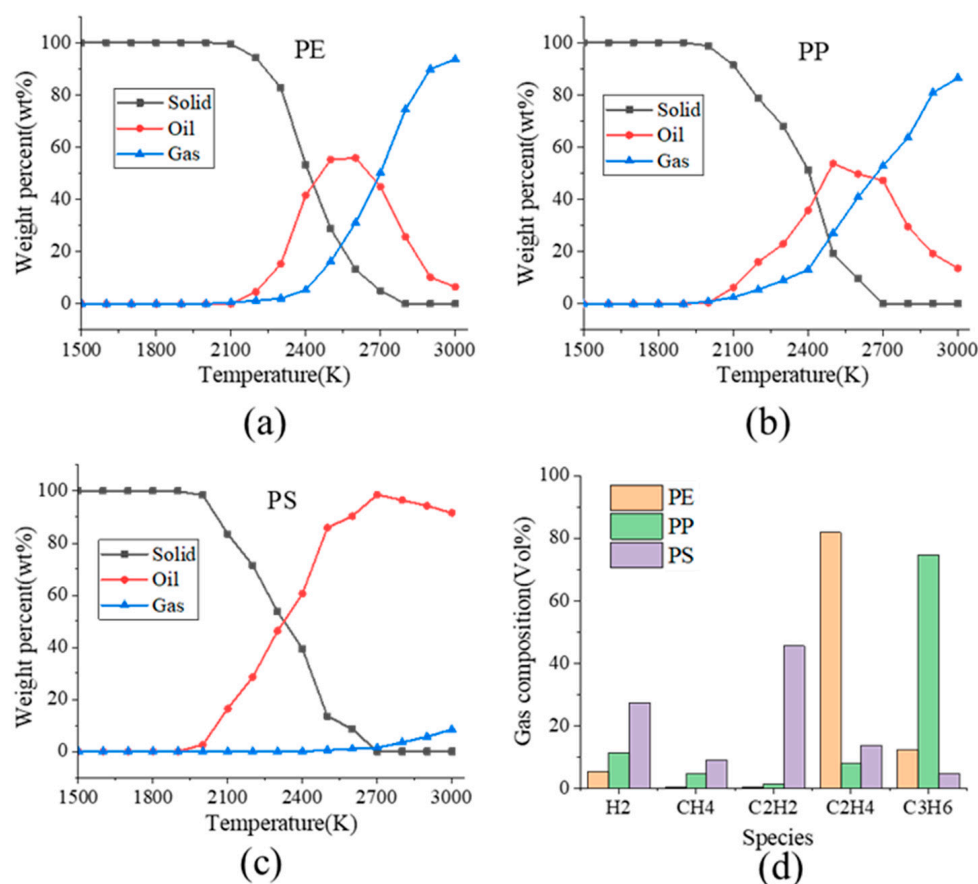


Figure 7. (a) Distribution of pyrolysis products for PE; (b) Distribution of pyrolysis products for PP; (c) Distribution of pyrolysis products for PS; (d) Gaseous products of PE, PP, PS.

3.2.4. Pyrolysis Mechanism of the Three Plastics

The pyrolysis process of the three plastics was observed at the micro-atomic level using ReaxFF-MD simulation and the results show that the process follows a common sequence where the polymer is dissociated to the polymer monomer and, then, to the gas molecule. Figure 8 shows the pyrolysis paths of the three plastics. Xuan et al. have carried out 50 independent simulations on the dissociation of a single molecular PE chain, and showed that all reactions begin with C–C bond breaking, and the initial dissociation position of a PE chain is random [28]. The C–C bond can break at different positions, resulting in some shorter chains. Then, after the initial C–C bond fracture of the polymer, the monomer appears in large numbers by terminal dissociation. The monomer structure continues to undergo free radical reactions, such as bond fracture and binding, intramolecular dehydrogenation and intermolecular dehydrogenation, to generate more stable gas molecules.

The breaking of the monomer connecting bond is critical in the polymer degradation process. The length of the monomer connecting bond is different due to the structural difference. Figure 9 shows the calculated lengths of the monomer connecting bonds at different positions in the chain for the three plastics. The $L(m, n)$ represents the length of the connecting bonds between the m and n monomers. The longer the bond length between the monomers, the weaker the connecting bond, which means that the bond is easier to break. Therefore, PS is easier to dissociate than PP and PE, which is consistent with the thermal weight loss.

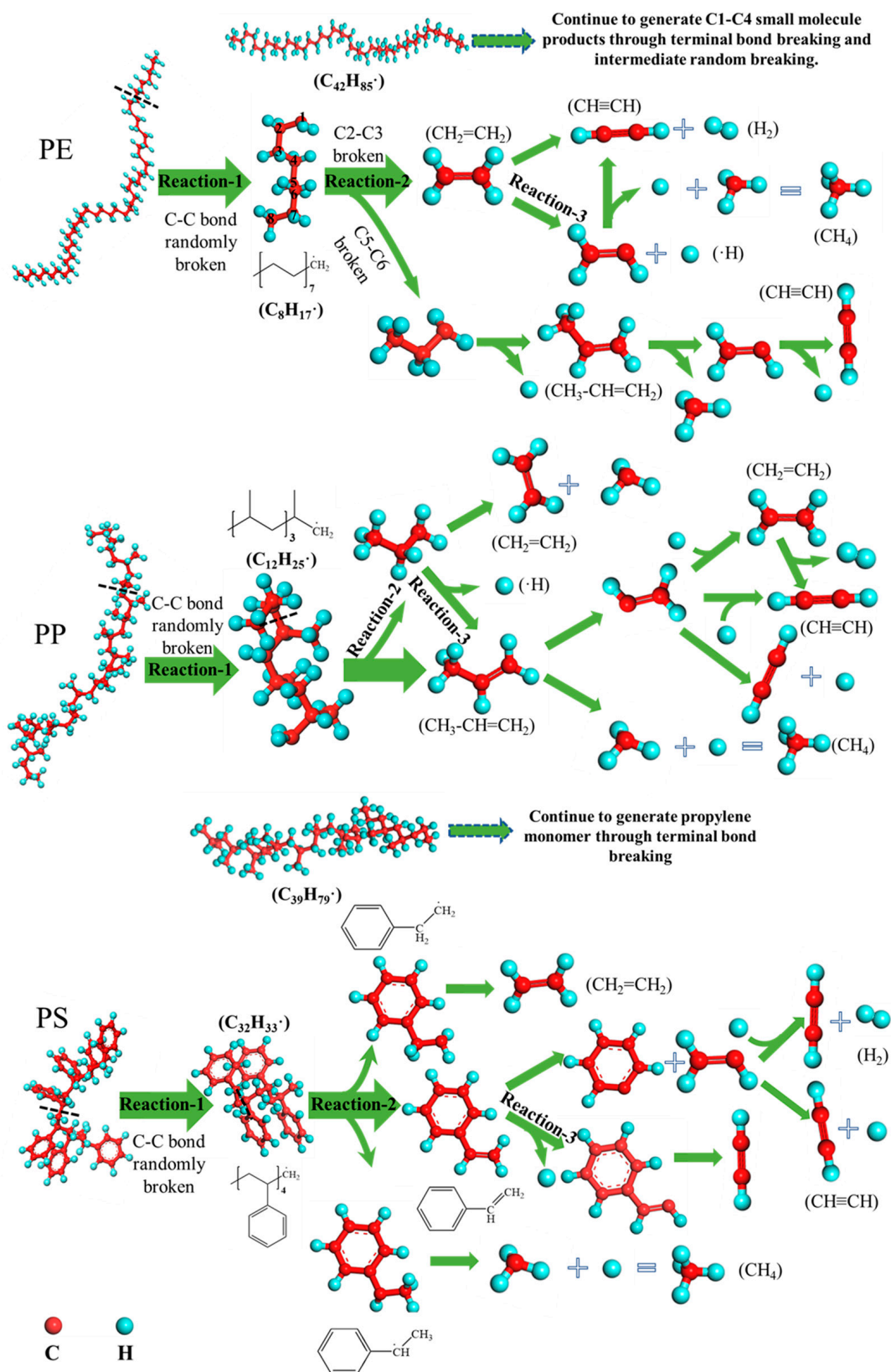


Figure 8. Pyrolysis mechanism and gas generation of the three plastics (Reaction-1: the initial bond breaking reaction, Reaction-2: the terminal dissociation to monomer reaction, Reaction-3: the monomer dehydrogenation reaction).

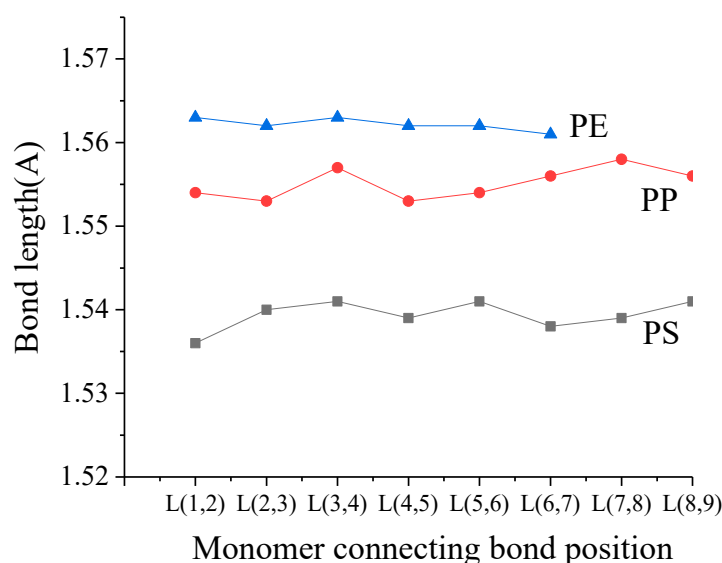


Figure 9. Bond lengths for different monomer connecting bonds in the three plastics (Å).

3.3. Study on Steam Gasification Mechanism using DFT

The common degradation sequence of the three polymers is the long polymer chain dissociates to the polymer monomer and, then, to the gas molecule. Therefore, we calculated the average bond energy for the main reactions in the pyrolysis process. As shown in Figure 9, Reaction-1 is the initial C–C bond breaking reaction, Reaction-2 is the terminal dissociation to monomer reaction and Reaction-3 is the monomer dehydrogenation reaction. It can be seen from Figure 10 that the energy barrier in monomer dehydrogenation is the highest and the monomer dissociation from the end of the chain occurs relatively easily. Comparing the different plastics, the sequence of the dissociation bond energy is in accordance with the energy barrier in the kinetic analysis. For all the three reactions, the bond energy for PE is the highest, while PS is the lowest, which indicates that PS is more prone to dissociation reaction than PE and PP plastics. This is mainly due to the existence of the benzene ring structure in its side chain, which intensifies the asymmetry of the main chain in the polymer and, thus, is more prone to the bond breaking reaction.

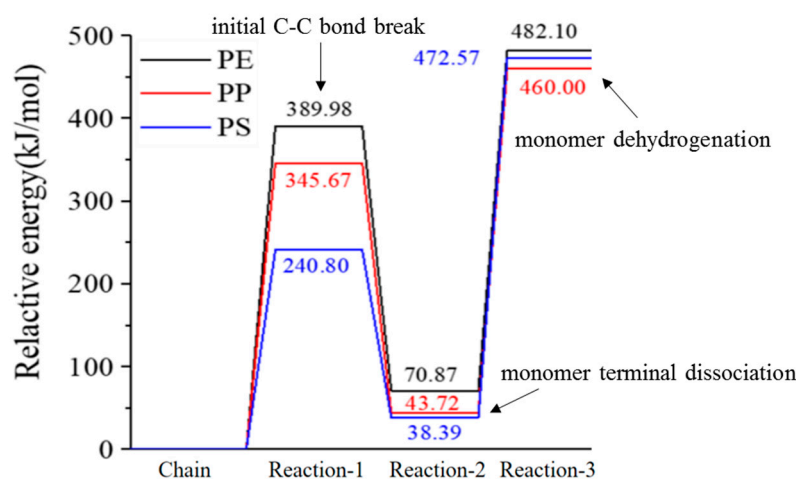


Figure 10. Bond energy for the main reactions during pyrolysis of the three plastics.

4. Conclusions

The reaction kinetics and pyrolysis mechanism of three waste plastics, PE, PP and PS, were explored using a TG experiment and ReaxFF-MD simulation. The non-isothermal methods, namely the Kissinger and Malek plus CR methods, were used to analyze the

experimental data, while the pyrolysis reaction process was revealed by ReaxFF-MD and DFT at the molecular level.

- (1) The kinetics obtained by the different methods is consistent with the 5% error. The thermal decomposition stability of the three plastics is ranked as PS < PP < PE. The reaction mechanism function for plastic pyrolysis is random nucleation and growth of the nuclei model.
- (2) The pyrolysis process of PE and PP is similar in that the oil and gas products are produced at the same time, and then the oil can crack later at a higher temperature. However, for PS, after the dissociation of the polymer, only about 2% of the aromatic rings can further dissociate into small gas molecules. The pyrolysis product from PS is almost completely oil.
- (3) The pyrolysis process of the three plastics all follows the dissociation sequence of polymer to polymeric monomer and, then, to the gas molecules. Due to the difference in the monomer structure, the bond strength between the monomers is different. The length of the monomer connecting bond ranks as PS > PP > PE. Based on the DFT calculation, the required dissociation energy for the critical reaction during pyrolysis is found to be PS < PP < PE. The results on the bond length and bond energy microscopically explain the sequence of the activation energy and thermal stability.

Supplementary Materials: The following supporting information can be downloaded at: <https://www.mdpi.com/article/10.3390/pr11092764/s1>, Figure S1: Fitting theoretical and experimental curves under Mark method of PE, PP and PS plastics; Table S1: 20 kinetic mechanism function models of solid pyrolysis [11].

Author Contributions: Writing—original draft, W.X.; Writing—review & editing, S.Y. and Y.D. All authors have read and agreed to the published version of the manuscript.

Funding: This work is supported by the National Natural Science Foundation of China (52276098) and the Fundamental Research Funds for the Central Universities (FRF-IDRY-22-022).

Data Availability Statement: Not applicable.

Conflicts of Interest: The authors declare no conflict of interest.

References

1. Laskar, N.; Kumar, U. Plastics and microplastics: A threat to environment. *Environ. Technol. Innov.* **2019**, *14*, 100352. [CrossRef]
2. Plastics—The Facts 2019. An Analysis of European Plastics Production, Demand and Waste Data. 2019. Available online: <https://plasticseurope.org/wp-content/uploads/2021/10/2019-Plastics-the-facts.pdf> (accessed on 28 August 2023).
3. Janajreh, I.; Adeyemi, I.; Elagroudy, S. Gasification feasibility of polyethylene, polypropylene, polystyrene waste and their mixture: Experimental studies and modeling. *Sustain. Energy Technol. Assess.* **2020**, *39*, 100684. [CrossRef]
4. Shen, M.; Huang, W.; Chen, M.; Song, B.; Zeng, G.; Zhang, Y. (Micro)plastic crisis: Un-ignorable contribution to global greenhouse gas emissions and climate change. *J. Clean. Prod.* **2020**, *254*, 120138. [CrossRef]
5. Sakthipriya, N. Plastic waste management: A road map to achieve circular economy and recent innovations in pyrolysis. *Sci. Total Environ.* **2022**, *809*, 151160.
6. Sharuddin, S.D.A.; Abnisa, F.; Daud, W.M.A.W.; Aroua, M.K. Pyrolysis of plastic waste for liquid fuel production as prospective energy resource. *Mater. Sci. Eng.* **2018**, *334*, 012001. [CrossRef]
7. Demirbas, A. Pyrolysis of municipal plastic wastes for recovery of gasoline-range hydrocarbons. *J. Anal. Appl. Pyrolysis* **2004**, *72*, 97–102. [CrossRef]
8. Yousef, S.; Eimontas, J.; Striugas, N.; Zakarauskas, K.; Praspaliauskas, M.; Abdelnaby, M.A. Pyrolysis kinetic behavior and TG-FTIR-GC-MS analysis of metallised food packaging plastics. *Fuel* **2020**, *282*, 118737. [CrossRef]
9. Hujuri, U.; Ghoshal, A.K.; Gumma, S. Modeling pyrolysis kinetics of plastic mixtures. *Polym. Degrad. Stab.* **2008**, *93*, 1832–1837. [CrossRef]
10. Zhu, Y.; An, J.; Chang, H.; Wang, X.-F.; Zhou, J.; Ding, L.; Zhang, X.-L. An analytical method for overlapping of the melting and decomposition of 2-oximemalononitrile. *J. Therm. Anal. Calorim.* **2021**, *146*, 1803–1809. [CrossRef]
11. Mortezaeikia, V.; Tavakoli, O.; Khodaparast, M.S. A review on kinetic study approach for pyrolysis of plastic wastes using thermogravimetric analysis. *J. Anal. Appl. Pyrolysis* **2021**, *160*, 105340. [CrossRef]
12. Pan, J.; Jiang, H.; Qing, T.; Zhang, J.; Tian, K. Transformation and kinetics of chlorine-containing products during pyrolysis of plastic wastes. *Chemosphere* **2021**, *284*, 131348. [CrossRef] [PubMed]

13. He, X.-c.; Chen, D.-z. ReaxFF MD study on the early stage co-pyrolysis of mixed PE/PP/PS plastic waste. *J. Fuel Chem. Technol.* **2022**, *50*, 346–356. [[CrossRef](#)]
14. Hu, Q.; Tang, Z.; Yao, D.; Yang, H.; Shao, J.; Chen, H. Thermal behavior, kinetics and gas evolution characteristics for the co-pyrolysis of real-world plastic and tyre waste. *J. Clean. Prod.* **2020**, *260*, 121102. [[CrossRef](#)]
15. Singh, S.; Patil, T.; Tekade, S.P.; Gawande, M.B.; Sawarkar, A.N. Studies on individual pyrolysis and co-pyrolysis of corn cob and polyethylene: Thermal degradation behavior, possible synergism, kinetics, and thermodynamic analysis. *Sci. Total Environ.* **2021**, *783*, 147004. [[CrossRef](#)] [[PubMed](#)]
16. Van Duin, A.C.T.; Dasgupta, S.; Lorant, F.; Goddard, W.A. ReaxFF: A reactive force field for hydrocarbons. *J. Phys. Chem. A* **2001**, *105*, 9396–9409. [[CrossRef](#)]
17. Agrawalla, S.; Van Duin, A.C.T. Development and Application of a ReaxFF Reactive Force Field for Hydrogen Combustion. *J. Phys. Chem. A* **2011**, *115*, 960–972. [[CrossRef](#)]
18. Liu, S.; Wei, L.; Zhou, Q.; Yang, T.; Li, S.; Zhou, Q. Simulation strategies for ReaxFF molecular dynamics in coal pyrolysis applications: A review. *J. Anal. Appl. Pyrolysis* **2023**, *170*, 105882. [[CrossRef](#)]
19. Castro-Marcanao, F.; Kamath, A.M.; Russo, M.F., Jr.; van Duin, A.C.T.; Mathews, J.P. Combustion of an Illinois No. 6 coal char simulated using an atomistic char representation and the ReaxFF reactive force field. *Combust. Flame* **2012**, *159*, 1272–1285. [[CrossRef](#)]
20. Kwon, H.; Lele, A.; Zhu, J.; McEnally, C.S.; Pfefferle, L.D.; Xuan, Y.; van Duin, A.C.T. ReaxFF-based molecular dynamics study of bio-derived polycyclic alkanes as potential alternative jet fuels. *Fuel* **2020**, *279*, 118548. [[CrossRef](#)]
21. Wen, Y.; Xie, Y.; Jiang, C.; Li, W.; Hou, Y. Products distribution and interaction mechanism during co-pyrolysis of rice husk and oily sludge by experiments and reaction force field simulation. *Bioresour. Technol.* **2021**, *329*, 124822. [[CrossRef](#)]
22. Zheng, M.; Wang, Z.; Li, X.; Qiao, X.; Song, W.; Guo, L. Initial reaction mechanisms of cellulose pyrolysis revealed by ReaxFF molecular dynamics. *Fuel* **2016**, *177*, 130–141. [[CrossRef](#)]
23. Liu, Q.; Liu, S.; Lv, Y.; Hu, P.; Huang, Y.; Kong, M.; Li, G. Atomic-scale insight into the pyrolysis of polycarbonate by ReaxFF-based reactive molecular dynamics simulation. *Fuel* **2021**, *287*, 119484. [[CrossRef](#)]
24. Batuer, A.; Chen, D.; He, X.; Huang, Z. Simulation methods of cotton pyrolysis based on ReaxFF and the influence of volatile removal ratio on volatile evolution and char formation. *Chem. Eng. J.* **2021**, *405*, 126633. [[CrossRef](#)]
25. Liu, X.; Lia, X.; Liu, J.; Wang, Z.; Kong, B.; Gong, X.; Yang, X.; Lin, W.; Guo, L. Study of high density polyethylene (HDPE) pyrolysis with reactive molecular dynamics. *Polym. Degrad. Stab.* **2014**, *104*, 62–70. [[CrossRef](#)]
26. Xu, Z.; Xie, Q.; Chen, C.; Jiang, X. Molecular dynamics simulation of converting waste polyethylene (PE) to chemicals and fuels under non-isothermal and isothermal conditions. *Polym. Degrad. Stab.* **2023**, *208*, 110249. [[CrossRef](#)]
27. Wang, Y.; Li, Y.; Zhang, C.; Yang, L.; Fan, X.; Chu, L. A study on co-pyrolysis mechanisms of biomass and polyethylene via ReaxFF molecular dynamic simulation and density functional theory. *Process Saf. Environ. Prot.* **2021**, *150*, 22–25. [[CrossRef](#)]
28. Hong, D.; Li, P.; Si, T.; Guo, X. ReaxFF simulations of the synergistic effect mechanisms during co-pyrolysis of coal and polyethylene/polystyrene. *Energy* **2021**, *218*, 119553. [[CrossRef](#)]
29. Xuan, W.; Wang, H.; Yan, S.; Xia, D. Exploration on the steam gasification mechanism of waste PE plastics based on ReaxFF-MD and DFT methods. *Fuel* **2022**, *315*, 123121. [[CrossRef](#)]
30. Anuar Sharuddin, S.D.; Abnisa, F.; Wan, W.; Aroua, M.K. A review on pyrolysis of plastic wastes. *Energy Convers. Manag.* **2016**, *115*, 308–326. [[CrossRef](#)]
31. Al-Salem, S.M.; Antelava, A.; Constantinou, A.; Manos, G.; Dutta, A. A review on thermal and catalytic pyrolysis of plastic solid waste (PSW). *J. Environ. Manag.* **2017**, *197*, 177–198. [[CrossRef](#)]
32. Kissinger, H.E. Variation of peak temperature with heating rate in differential thermal analysis. *Res. Natl. Bur. Od. Stand.* **1956**, *57*, 217–221. [[CrossRef](#)]
33. Hu, R.; Gao, S.; Zhao, F. *Thermal Analysis Kinetics*; Science Press: Beijing, China, 2008.
34. Málek, J. The kinetic-analysis of nonisothermal data. *Thermochim. Acta* **1992**, *200*, 257–269. [[CrossRef](#)]
35. Coats, A.W.; Redfern, J.P. Kinetic parameters from thermogravimetric data. *Nature* **1996**, *201*, 68–69. [[CrossRef](#)]
36. Knyazev, V.D. Effects of Chain Length on the Rates of C-C Bond Dissociation in Linear Alkanes and Polyethylene. *J. Phys. Chem. A* **2007**, *111*, 3875–3883. [[CrossRef](#)] [[PubMed](#)]
37. Smitha, K.D.; Brunsb, M.; Stoliarov, S.I.; Nyden, M.R.; Ezekoye, O.A.; Westmoreland, P.R. Assessing the effect of molecular weight on the kinetics of backbone scission reactions in polyethylene using Reactive Molecular Dynamics. *Polymer* **2011**, *52*, 3104–3111. [[CrossRef](#)]
38. Evans, D.J.; Holian, B.L. The Nose-Hoover Thermostat. *J. Phys. Chem.* **1985**, *83*, 4069–4074. [[CrossRef](#)]
39. Li, W.; Yu, S.; Zhang, L.; Chen, J.; Cao, W.; Lan, Y. ReaxFF molecular dynamics simulations of n-eicosane reaction mechanisms during pyrolysis and combustion. *Int. J. Hydrogen Energy* **2021**, *46*, 38854–38870. [[CrossRef](#)]
40. Wang, Q.; Wang, J.; Li, J.; Tan, N.-X.; Li, X.-Y. Reactive molecular dynamics simulation and chemical kinetic modeling of pyrolysis and combustion of n-dodecane. *Combust. Flame* **2011**, *158*, 217–226. [[CrossRef](#)]
41. Lee, C.; Yang, W.; Parr, R.G. Development of the Colic-Salvetti correlation-energy formula into a functional of the electron density. *Phys. Rev. B* **1988**, *37*, 785–789. [[CrossRef](#)]
42. Mastellone, M.L.; Zaccariello, L.; Arena, U. Co-gasification of coal, plastic waste and wood in a bubbling fluidized bed reactor. *Fuel* **2010**, *89*, 2991–3000. [[CrossRef](#)]

43. Wei, X.; Zhong, H.; Yang, Q. Studying the mechanisms of natural rubber pyrolysis gas generation using RMD simulations and TG-FTIR experiments. *Energy Convers. Manag.* **2019**, *189*, 143–152. [[CrossRef](#)]
44. Maite, A.; Gartzen, L.; Mainer, A.; Barbarias, I.; Arregi, A.; Aguado, R.; Bilbao, J.; Olazar, M. Styrene recovery from polystyrene by flash pyrolysis in a conical spouted bed reactor. *Waste Manag.* **2015**, *45*, 126–133.
45. Jan, N.; Ghulam, A.; Afzal, S.; Iqbal, M.; Khan, R.A.; Sirajuddin; Anwar, F.; Ullah, R.; Akhter, M.S. Fuel production from waste polystyrene via pyrolysis: Kinetics and products distribution. *Waste Manag.* **2019**, *88*, 236–247.
46. Qin, L.; Han, J.; Zhao, B.; Wang, Y.; Chen, W.; Xing, F. Thermal degradation of medical plastic waste by in-situ FTIR, TG-MS and TG-GC/MS coupled analyses. *J. Anal. Appl. Pyrolysis* **2018**, *136*, 132–145. [[CrossRef](#)]
47. Yan, S.; Xia, D.; Zhang, X.; Jiang, B. A complete depolymerization of scrap tire with supercritical water participation: A molecular dynamic simulation study. *Waste Manag.* **2019**, *93*, 83–90. [[CrossRef](#)]
48. Cheng, X.; Wang, Q.; Li, J.; Wang, J.B.; Li, X.Y. ReaxFF Molecular Dynamics Simulations of Oxidation of Toluene at High Temperatures. *J. Phys. Chem. A* **2012**, *116*, 9811–9818. [[CrossRef](#)]
49. Encinara, J.M.; González, J.F. Pyrolysis of synthetic polymers and plastic wastes. Kinetic study. *Fuel Process. Technol.* **2008**, *89*, 678–686. [[CrossRef](#)]

Disclaimer/Publisher’s Note: The statements, opinions and data contained in all publications are solely those of the individual author(s) and contributor(s) and not of MDPI and/or the editor(s). MDPI and/or the editor(s) disclaim responsibility for any injury to people or property resulting from any ideas, methods, instructions or products referred to in the content.